# PHOTOFRAGMENTATION DYNAMICS OF $H_2O_2$ AT 193 nm

Axel Ulrich GRUNEWALD, Karl-Heinz GERICKE and Franz Josef COMES

*Institut für Physikalische und Theoretische Chemie an der Universität Frankfurt am Main, Niederurseler Hang, D-6000 Frankfurt am Main 50, Federal Republic of Germany*

Received 16 September 1986

The photofragmentation dynamics of $H_2O_2$ at 193 nm have been analyzed by probing the OH products by Doppler spectroscopy using laser-induced fluorescence. The excess energy ($E_{av}$ = 417 kJ/mol) appears mostly as translational motion of the fragments with $f_t$ = 0.84. No vibrational excitation was observed ($f_v < 0.003$). The rotational state distribution is strongly inverted, peaking for $N''$ = 12 which results in $f_r$ = 0.16. Our results indicate that previously published rotational state distributions are not nascent in character, but are perturbed by rotational relaxation. Individual fragment recoil velocities obtained from Doppler lineshapes are $v$ = 4950 m $s^{-1}$ [OH($N''$ = 4)] and $v$ = 4550 m $s^{-1}$ [OH($N''$ = 10)]. The effective anisotropy parameter $\beta_{eff}$ is slightly negative at high $N''$ ($\beta_{eff}$ = 0.35 at $N''$ = 10).

## 1. Introduction

The tetraatomic $H_2O_2$ is a useful molecule for the study of photofragmentation processes and their dynamics. Photofragmentation of $H_2O_2$ leads to two molecular fragments which are chemically equivalent and which can both be monitored by the same spectroscopic techniques. Moreover, the spectroscopy of OH radicals is well known so that the internal state distribution of the fragments can be completely established.

The absorption spectrum of $H_2O_2$ in the UV is structureless and entirely continuous [1] which indicates a fast dissociation process. This makes the study of its photodissociation particularly suitable for extracting fragment vector properties using polarization and Doppler spectroscopy [2–4]. Photofragmentation at wavelengths longer than 172 nm leads to (electronic) ground state OH radicals [1]. At shorter wavelengths one of the OH fragments is produced in its first excited electronic state, $^2\Sigma^+$, which demonstrates the existence of a new dissociation channel at higher energies. Studies of the photodissociation at 157 nm and shorter wavelengths showed that the electronically excited fragments are formed with an inverted rotational state distribution [5]. Moreover, a strong rotational alignment is also observed [6].

At the longer wavelengths used to study $H_2O_2$ photodissociation, the OH fragments were observed using the sensitive LIF technique. Due to the high resolution of the applied dye lasers fine details such as spin state and $\Lambda$ state populations could be studied as well as the partitioning of the excess energy into the rotational and vibrational degrees of freedom of the fragments. The application of polarization and Doppler spectroscopy clearly demonstrated that on absorption of radiation at 266 and 248 nm the only excited electronic state is the $\tilde{A}\,^1A$ state of $H_2O_2$ [2–4].

Using the excitation wavelength of the ArF laser at 193 nm this picture of only one excited electronic state changes. The rotational state distribution was no longer representable by a Boltzmann-like distribution. Instead a bimodal rotational distribution was found indicating the excitation of more than one electronic state [7]. As in the case for the longer excitation wavelengths at 248 and 266 nm, no vibrational excitation of the fragments was observed and the bulk of the excess energy is transferred into fragment recoil translation.

In the present study, the measurement of the photofragmentation of $H_2O_2$ at 193 nm has been repeated. From the experimental conditions used in the earlier study [7] and from information obtained



0 009-2614/86/$ 03.50 

on the rotational relaxation of OH [8], it is expected that the previously reported rotational distribution does not represent collision-free conditions. This would have serious consequences for the population of fragments in low $J$ states, and any inversion in the nascent fragment rotational state distribution would vanish. The present results indicate the severe influence of rotational relaxation on the populations of fragment rotational states and show that there is in fact a strong inversion in the population of the OH rotational states.

In addition to the determination of the nascent internal state distribution, Doppler profile measurements have been carried out to obtain detailed information on the velocity of the recoiling OH photofragments.

## 2. Experimental

The reaction cell is made of stainless steel and was evacuated by diffusion pumps. The vessel is provided with two gas inlet systems allowing observation of the photodissociation process in the bulk as well as in a supersonic jet. In the present study the probe gas is continuously flowing through the cell at a pressure of typically 5 mTorr. The probe gas is 90% pure and is stored in a glass bulb. The gas flow can be regulated by a glass needle valve.

The photolysis is an ArF laser operating with a repetition frequency of 10 Hz. Inside the reaction cell, the dissociating laser beam has an energy of 5 mJ. The probe laser was a Nd–YAG-pumped frequency-doubled dye laser with a linewidth of 0.1 $cm^{-1}$, measured with an external UV etalon. No saturation effects on the LIF signals were observed when operating at an average pulse energy of 5 $\mu$J. Both laser beams are in the counterpropagating position. A set of baffles was installed to reduce stray light in the cell.

Photolysis of the parent molecules for probing the Doppler profiles of the fragments was achieved by operating both laser beams polarized with a parallel polarization direction and also parallel to the direction of the observation of fluorescence radiation which itself is perpendicular to both beam propagation directions. The detector is a photomultiplier with a bialkali cathode. The delay between the photolysis laser and the probe laser was set at 50 ns. Both laser beams were monitored with pyroelectric detectors. A minicomputer was used for data acquisition and to control the proper timing of the lasers, the detector system, and the wavelength setting of the probe laser.

## 3. Results and discussion

### 3.1. Internal state distribution

We observed in the photodissociation of $H_2O_2$ at 193 nm the production of two OH radicals which are formed exclusively in the $^2\Pi_{3/2,\,1/2}$ electronic ground state. This result agrees with a former single-photon investigation at 193 nm and indicates that two-photon absorption, to produce electronically excited OH radicals, has not taken place [9], because no emission from the OH $X\,^2\Sigma$ state could be found.

The OH photofragment distribution is probed by excitation of the $X\,^2\Pi \rightarrow A\,^2\Sigma^+$ band. Fig. 1 shows the LIF spectrum of this band for OH products generated by *unpolarized* photolysis light at 193 nm. The transitions were assigned on the basis of the work of Dieke and Crosswhite [10].

The relative population number of each quantum state was taken from the P, R, and Q main lines with no correction for alignment. The Q branch probes the $\Pi^-$ component of the $\Lambda$ doublet which for high rotation has the unpaired electron in a p$\pi$ orbital aligned parallel to the rotational vector $J_{OH}$ while the R and P branches analyze the $\Pi^+$ $\Lambda$ doublet which has the unpaired electron in a p$\pi$ orbital aligned perpendicular to $J_{OH}$. The population of the two $\Lambda$ components shows a weak dependence of the OH rotation with an increasing preference for the upper $\Lambda$ component.

The rotational population distribution $P(J_{OH}, v = 0)$ is shown in fig. 2 for both the $^2\Pi_{3/2}$ (squares) and the $^2\Pi_{1/2}$ (circles) spin systems. The population of a particular rotational state is given as an arithmetic mean of the $\Pi^-$ and $\Pi^+$ components. Within experimental error, the two spin components of the OH photofragments are statistically populated, and consequently the dissociation process does not distinguish between the two spin–orbit states. The rotational distribution is completely different from a Boltzmann form and cannot be characterized by a single "tem-

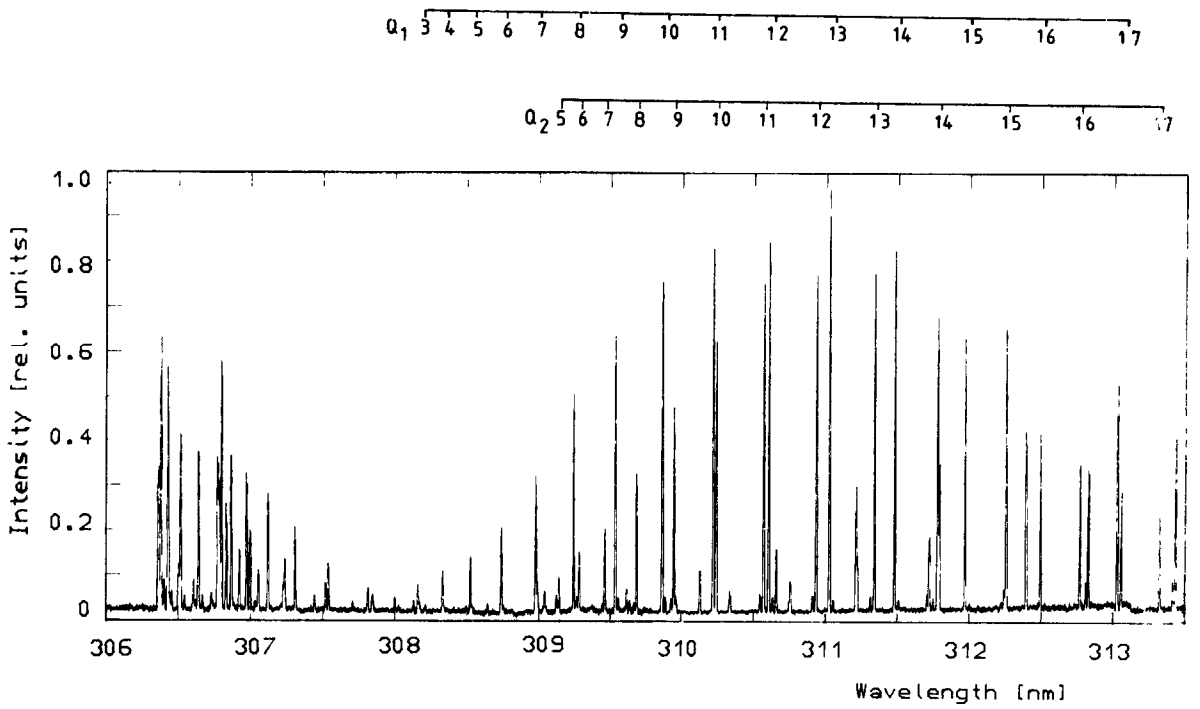


Fig. 1. A section of the (0,0) band of the excitation spectrum of OH($^2\Pi$) fragments generated by the photolysis of $H_2O_2$ at 193 nm. The photolysis and the probe laser beams were counterpropagated. Laser-induced fluorescence was detected perpendicular to the propagation direction of the laser beams. $P_{tot}$ = 5 mTorr; time delay between the two lasers was 50 ns.

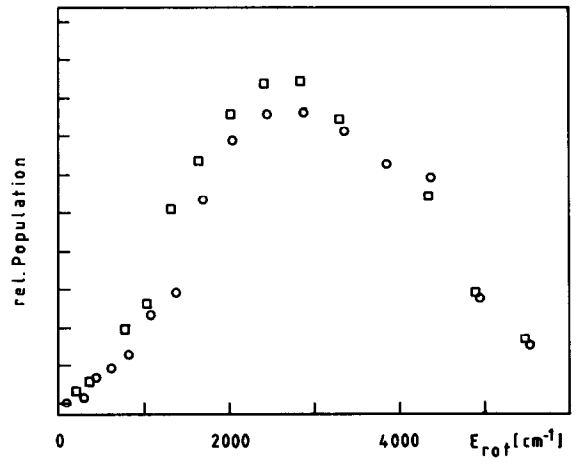


Fig. 2. Rotational state distribution of OH fragments from the photolysis of $H_2O_2$ at 193 nm with no corrections for alignment. Contributions from the two spin states are given by squares for the $^2\Pi_{3/2}$ and by circles for the $^2\Pi_{1/2}$ state.

perature" parameter. The distributions peak at the quantum number $N_{OH}$ = 12. All lower rotational states show a population inversion ‡. A comparison with pre-existing results for the photodissociation of $H_2O_2$ at 193 nm shows a remarkable difference for these lower rotational states. While we observe an increase in $P(J)/(2J+1)$ (for $J \leqslant 12$), Ondrey et al. [7] report a monotonic decrease. The difference in the observed rotational state distribution is caused by rotational relaxation processes which are known to be extremely fast for collisions of OH radicals with $H_2O$ [8]. We could reproduce the reported rotational distribution with a pressure of 100 mTorr and a delay time of 100 ns between photolyzing

‡ Any corrections from alignment effects will not significantly change the rotational state distribution, especially not for low $J$ values where the main deviation from the earlier reported results is observed. In the present case, the alignment effect will be reduced by the use of an unpolarized photolysis laser and by contributions from the $\tilde{A}\,^1A$ state in $H_2O_2$.

and analyzing laser beams. The procedure we chose to exclude rotational relaxation was to decrease the $H_2O_2/H_2O$ pressure until the observed OH photofragment rotational distribution remained unchanged. The population of lower OH rotational states was strongly affected when the total pressure was decreased from 100 to 5 mTorr.

Another complication in the investigation of the photodissociation of $H_2O_2$ may result from the presence of water in the $H_2O_2/H_2O$ solution and the possibility of $H_2O_2$ decomposition on the walls of the vacuum chamber because excitation of water to its lowest excited electronic $^1B_1$ state leads also to the production of an electronic ground state OH radical [11]. The absorption cross section of this process is much smaller than in the case of $H_2O_2$ but, in a different experiment, we could observe OH fragments originating from $H_2O$ parent molecules [12].

Fortunately, the OH radicals formed in the water photolysis exhibit a much lower translational velocity than those resulting from $H_2O_2$ fragmentation because the available energy is lower and most of the translational energy is carried by the H atom. Consequently a linewidth measurement easily distinguishes between OH radicals formed in the photolysis of $H_2O$ compared to those formed from $H_2O_2$. Since OH radicals from the $H_2O$ photolysis are formed with low rotational excitation, we determined the OH line profile for the $Q_1(4)$ line in the $X\,^2\Pi_{3/2}(v''=0) \rightarrow A\,^2\Sigma(v'=0)$ transition. The measured linewidth was $\Delta\nu = 1\ \mathrm{cm}^{-1}$. OH from the photolysis of water should exhibit a narrow line with a width of only $\Delta\nu = 0.25\ \mathrm{cm}^{-1}$, which in fact was observed when the water partial pressure was strongly increased [12]. The present data indicate, however, that the measurements were not influenced by the presence of water.

An inspection of the observed OH excitation spectrum above 312 nm, where the $v'' = 1 \rightarrow v' = 1$ band occurs, indicates that no vibrationally excited OH fragments can be found. This result is not surprising because the equilibrium bond length as well as the stretching frequency of OH in the parent $H_2O_2$ are comparable to those of the free radical. As the OH bond is not involved in the dissociation process, Franck–Condon predicts no vibrational excitation of the fragment. Based on the sensitivity of our experiment an upper limit of the $v'' = 1$ population is estimated to be 3%.

### 3.2. Energy partitioning

The total excess energy, $E_{av}$, which is available to the OH ($X\,^2\Pi$) photofragments is determined by the binding energy, $D_0 = 207$ kJ/mol, the photon energy of the photolyzing laser light, $h\nu = 619.1$ kJ/mol, and the initial energy $E_{int}(H_2O_2)$ of the parent:

$$E_{av} = h\nu + E_{int}(H_2O_2) - D_0 \,. \tag{1}$$

At room temperature, the parent hydrogen peroxide molecules have an average $\frac{3}{2}RT$ rotational energy, $E_r$, and a lower amount of vibrational energy, $E_v$, which mainly originates from the $\nu_4$ torsional mode:

$$E_{int}(H_2O_2) = E_v(H_2O_2) + E_r(H_2O_2) = 4.8\ \mathrm{kJ/mol}\,. \tag{2}$$

Thus, the total energy available for excitation of the two OH fragments is

$$E_{av} = 476.9\ \mathrm{kJ/mol}\,. \tag{3}$$

The fraction of energy which is transferred into one OH fragment is given by

$$f_r = \langle E_r\rangle/E_{av} = \sum_J P(J)E_r(J)/E_{av} = 0.08\,, \tag{4}$$

where $P(J)$ is the normalized population of the rotational state $J$ and $E_r(J)$ is the rotational energy.

Since *two* OH photoproducts are formed without vibrational excitation, the fraction of energy which is released into fragment translation is given by

$$f_t = 1 - 2f_r = 0.84\,, \tag{5}$$

a consequence of conservation of energy.

The observed energy partitioning implies that very fast photofragments with a narrow velocity distribution should be expected. Based on the energy $E_t$ released into translation, $E_t = f_t E_{av} = 350$ kJ/mol, the most probable OH recoil velocity is calculated to be

$$v_{OH} = (E_t/m_{OH})^{1/2} = 4540\ \mathrm{m/s}\,. \tag{6}$$

With this large OH fragment centre-of-mass velocity in comparison to the small probe laser linewidth and parent Doppler motion, it becomes possible to examine the fragment angular recoil and velocity distribution by Doppler spectroscopy.

### 3.3. OH photofragment Doppler profiles

The nascent OH fragment internal state distribu-

tions have been determined under collision-free conditions. In addition, Doppler profile measurements can give information about the product recoil velocity and vector properties of the dissociation process. The transition moment of a photoselected parent molecule is preferentially aligned parallel to the electric field vector, $E_D$, of the exciting polarized laser radiation. This anisotropy will be carried over to the photofragment motion if the dissociation of the parent is faster than the molecular rotation; at very long times, the internal motion of the parent will dominate the measurable fragment translational anisotropy and rotational alignment. In the case of the photolysis of hydrogen peroxide at 193 nm, a well-structured angular distribution can be expected because most of the available energy appears in OH recoil, and the smooth absorption spectrum implies a fast dissociation process.

For an electric dipole transition, the Doppler line shape function is given by

$$g(x_D) \sim (1/2\Delta\nu_D)[1 + \beta_{eff} P_2(\cos\theta) P_2(x_D)] , \quad (7)$$

where $\theta$ is the angle between the electric vector, $E_D$, of the dissociating light and the direction at which the fragment is analyzed; $P_2(\cos\theta)$ is the second Legendre polynomial in $\cos\theta$, $\Delta\nu_D$ is the maximum Doppler shift and $x_D = (\nu - \nu_0)/\Delta\nu_D$ is the relative displacement from the OH absorption line center $\nu_0$. The parameter $\beta_{eff}$ contains information on various vector correlations between the direction of recoil, the translational motion, the angular momentum of fragments, and the transition dipole moment in the parent molecule (for details see ref. [3]).

The recoil Doppler broadened line profile obtained for the $Q_1(10)$ line is shown in fig. 3. The propagation direction of the analyzing dye laser beam was perpendicular to the $E_D$ vector of the dissociating excimer laser light at 193 nm which corresponds to geometry IV of ref. [3] ($E_a \| E_D \| \hat{z}$). The solid line shows the best-fit profile $g(x_D)$ for a single recoil velocity of the OH fragments with suitable convolution of a Gaussian profile to account for the probe laser linewidth and parent Doppler motion [2]. The value found for the Doppler shift is $\Delta\tilde{\nu}_D = 0.49 \pm 0.02$ $cm^{-1}$ which corresponds to an OH recoil velocity of $v_{OH}(N'' = 10) = 4550 \pm 190$ m/s.

In addition to the $Q_1(10)$ line, we also analyzed the Doppler profile of the $Q_1(4)$ line. A least-squares fit procedure according to eq. (7) yields a value of

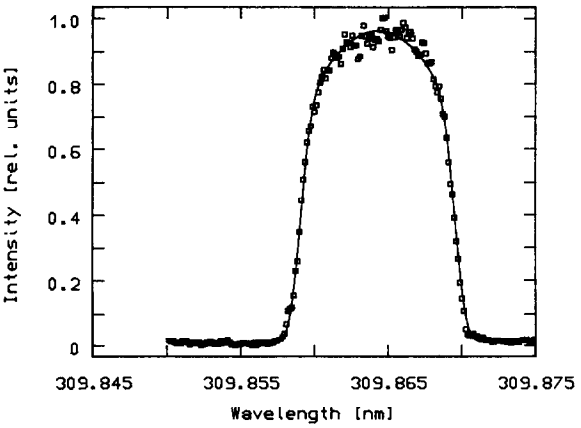


Fig. 3. Doppler lineshape of the $Q_1(10)$ transition of the (0,0) band of OH ($X^2\Pi$). The effective symmetry parameter $\beta_{eff} = 0.35$ has been computed by fitting the experimental data using eq. (7) and convoluted with a 300 K thermal motion of $H_2O_2$ ($\Delta\tilde{\nu} = 0.069$ $cm^{-1}$) and a Gaussian laser profile ($\Delta\tilde{\nu}_L = 0.1$ $cm^{-1}$). The laser beams were counterpropagated and linearly polarized parallel to each other with the $E$ vector parallel to the direction of observation. The photomultiplier accepted all polarizations equally.

$\Delta\tilde{\nu}_D = 0.54 \pm 0.03$ $cm^{-1}$ for the Doppler width. The corresponding OH recoil velocity, $v_{OH}(N'' = 4) = 4990 \pm 280$ m/s, is higher than the velocity of those fragments which are formed in the $N'' = 10$ rotational state.

The partner OH fragment which is formed simultaneously with the observed OH product must have the same translational energy in the center-of-mass system. Thus, the total kinetic energy $2E_{kin} = mv_{OH}^2$ of coincident partner OH fragments is $2E_{kin}(N'' = 4) = 423 \pm 47$ kJ/mol for the OH probed via the $Q_1(4)$ line and $2E_{kin}(N'' = 10) = 352 \pm 28$ kJ/mol for OH formed in the $N'' = 10$ rotational state ($Q_1(10)$ line).

For a comparison of these values with the total available energy, $E_{av} = 417$ kJ/mol, the rotational energy of the observed OH fragment has to be added. The remaining energy has to be carried by the rotational excitation of the partner product.

The rotational energy, $E_r$, of the fragment probed by the $Q_1(10)$ line is $E_r(N'' = 10) = 24$ kJ/mol [13]. Consequently, the simultaneously formed OH fragment must also have a significant amount of rotational energy to fulfill the law of conservation of energy,

$$E_{av} = 2E_{kin} + E_r(OH_1) + E_r(OH_2) .$$

The rotational energy of the OH product, probed by the $Q_1(4)$ line is, $E_r(N'' = 4) = 4$ kJ/mol. Since this energy and the measured translational energy already agree with the total available energy within experimental error, the OH partner fragment must also be formed with low rotational excitation.

The linewidth measurements imply a correlation between the rotation of the two simultaneously formed fragments, $N(OH_1)$ and $N(OH_2)$. However, more accurate measurements are necessary to investigate these microscopic reaction probabilities for the formation of coincident partner products.

The anisotropy parameter $\beta_{eff}$ obtained by fitting the observed Doppler profile of fig. 3 to the function $g(x_D)$ (eq. (7)) is given by $\beta_{eff} = 0.35 \pm 0.10$. If the translational and rotational motion of the recoiling photofragments are not correlated with each other, then $\beta_{eff}$ describes only the vector correlation between the transition dipole moment in the parent molecule and the translational motion $v$ of the recoiling fragment [3].

A negative value of $\beta_{eff}$ implies that the angular distribution peaks in the direction perpendicular to the electric vector. The limiting value of $\beta_{eff} = -1$ would correspond to an excitation of a (4b) electron to the antibonding (5b) orbital:

$$\tilde{X}\,^1A[(4a)^2(5a)^2(4b)^2] + h\nu$$

$$\rightarrow \tilde{A}\,^1A[(4a)^2(5a)^2(4b)(5b)]\,,$$

with the transition moment lying along the $C_2$ axis [14]. This transition is the only one which was involved in the photodissociation of $H_2O_2$ at 266 nm and 248 nm [2–4].

However, at 193 nm, $\tilde{X}\,^1A \rightarrow \tilde{B}\,^1B[(4a)^2(5a)(4b)^2(5b)]$ may also be excited; this transition has a strong component of the transition moment along the O–O axis [14]. Excitation of this $^1B$ state will result in a positive $\mu$–$v$ correlation coefficient. Therefore, any contribution of the $^1B$ state to an excitation of $H_2O_2$ increases the anisotropy parameter $\beta_{eff}$. Since $\beta_{eff}$ is also influenced by parent rotation and $v$–$J$ correlation, it cannot be decided at present to what extent the $\tilde{B}\,^1B$ state of electronically excited $H_2O_2$ is involved in the fragmentation process.

Work is in progress on the photolysis of jet cooled $H_2O_2$ at 193 nm, and we hope to study all observable OH excitation line profiles at different detection geometries [15].

Bersohn and Shapiro [16] studied the dissociation of $H_2O_2$ from low-lying excited electronic states by classical trajectory calculations, where parameters in the excited state functions were chosen to fit the observed OH rotational state distribution and to be consistent with the electronic spectrum. Since the nascent rotational state distribution, observed in the present experiment, is remarkably different from the bimodal distribution observed by Ondrey et al. [7], some of the parameters, used to describe the excited electronic state of $H_2O_2$, should be modified.

A model for the observed rotational state distribution may be also given by the "rotational reflection principle" [17] which establishes a direct relationship between the bound state wavefunction of the parent, the anisotropy of the repulsive potential, and the final rotational state distribution. The calculated distributions are usually smooth and inverted as in the case of the photodissociation of hydrogen peroxide at 193 nm.

## Acknowledgement

The work has been performed as part of a program of the Deutsche Forschungsgemeinschaft. Financial support is gratefully acknowledged.

## References

[1] M. Suto and L.C. Lee, Chem. Phys. Letters 98 (1983) 152.
[2] S. Klee, K.-H. Gericke and F.J. Comes, J. Chem. Phys. 85 (1986) 40.
[3] K.-H. Gericke, S. Klee, F.J. Comes and R.N. Dixon, J. Chem. Phys., to be published.
[4] M.P. Docker, A. Hodgson and J.P. Simons, Chem. Phys. Letters 128 (1986) 264; Faraday Discussions Chem. Soc., to be published.
[5] H. Gölzenleuchter, K.-H. Gericke, F.J. Comes and P.F. Linde, Chem. Phys. 89 (1984) 93; K.H. Becker, W. Groth and D. Kley, Z. Naturforsch. 20a (1965) 748.
[6] H. Gölzenleuchter, K.-H. Gericke and F.J. Comes, to be published.
[7] G.S. Ondrey, N. van Veen and R. Bersohn, J. Chem. Phys. 78 (1983) 3732; A. Jacobs, K. Kleinermans, H. Kluge and J. Wolfrum, J. Chem. Phys. 79 (1983) 3162.
[8] K.-H. Gericke and F.J. Comes, Chem. Phys. 65 (1982) 113.

[9] C.B. McKendrick, E.A. Kerr and J.P.T. Wilkinson, J. Phys. Chem. 88 (1984) 3930;
H. Gölzenleuchter, K.-H. Gericke and F.J. Comes, Chem. Phys. Letters 116 (1985) 60.
[10] G.H. Dieke and H.M. Crosswhite, J. Quant. Spectry. Radiative Transfer 2 (1962) 97.
[11] P. Andresen, G.S. Ondrey, B. Titze and E.W. Rothe, J. Chem. Phys. 80 (1984) 2548.
[12] U.A. Grunewald, K.-H. Gericke and F.J. Comes, to be published.
[13] M. Nuss, K.-H. Gericke and F.J. Comes, J. Quant. Spectry. Radiative Transfer 27 (1982) 191.
[14] C. Chevaldonnet, H. Cardy and A. Dargelos, Chem. Phys. 102 (1986) 55.
[15] U.A. Grunewald, K.-H. Gericke and F.J. Comes, to be published.
[16] R. Bersohn and M. Shapiro, J. Chem. Phys. 85 (1986) 1396.
[17] R. Schinke, J. Phys. Chem. 90 (1986) 1742.